Supporting Information

Network topology and cavity confinement-controlled diastereoselectivity in cyclopropanation reactions catalyzed by porphyrin-based MOFs

Konstantin Epp,[a] Bart Bueken,[b] Benjamin J. Hofmann,[c] Mirza Cokoja,[a] Karina Hemmer,[a] Dirk De Vos[b] and Roland A. Fischer[a,*]

[a] Chair of Inorganic and Metal-Organic Chemistry, Catalysis Research Center and Department of Chemistry, Technical University of Munich, Ernst-Otto-Fischer-Straße 1, D-85748 Garching bei München, Germany.

[b] Centre for Surface Chemistry and Catalysis, Department of Microbial and Molecular Systems (M^2S), KU Leuven, Celestijnenlaan 200F p.o. box 2461, 3001 Leuven, Belgium.

[c] Molecular Catalysis, Catalysis Research Center and Department of Chemistry, Technical University of Munich, Ernst-Otto-Fischer-Straße 1, D-85748 Garching bei München, Germany.

Table of contents

1. UV-Vis spectroscopy

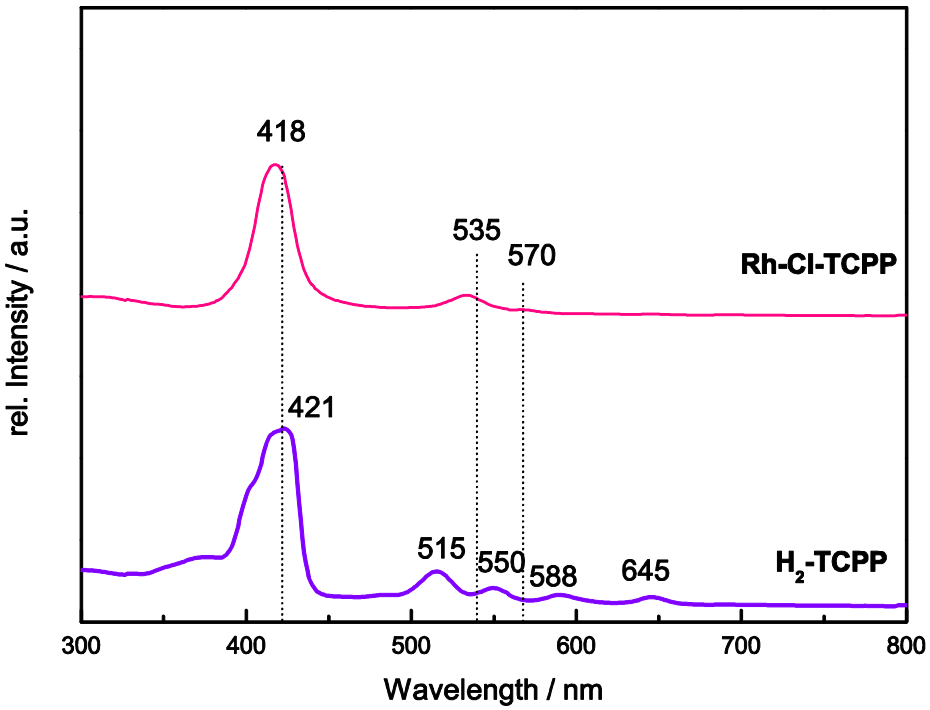

Figure S1. UV-VIS spectra of molecular free base 5,10,15,20-(tetra-4-carboxyphenyl)porphyrin (H_2TCPP) in comparison to its Rh-metalated analog (Rh-Cl-TCPP) measured in DMSO.

2. Energy dispersive spectroscopy (EDS)

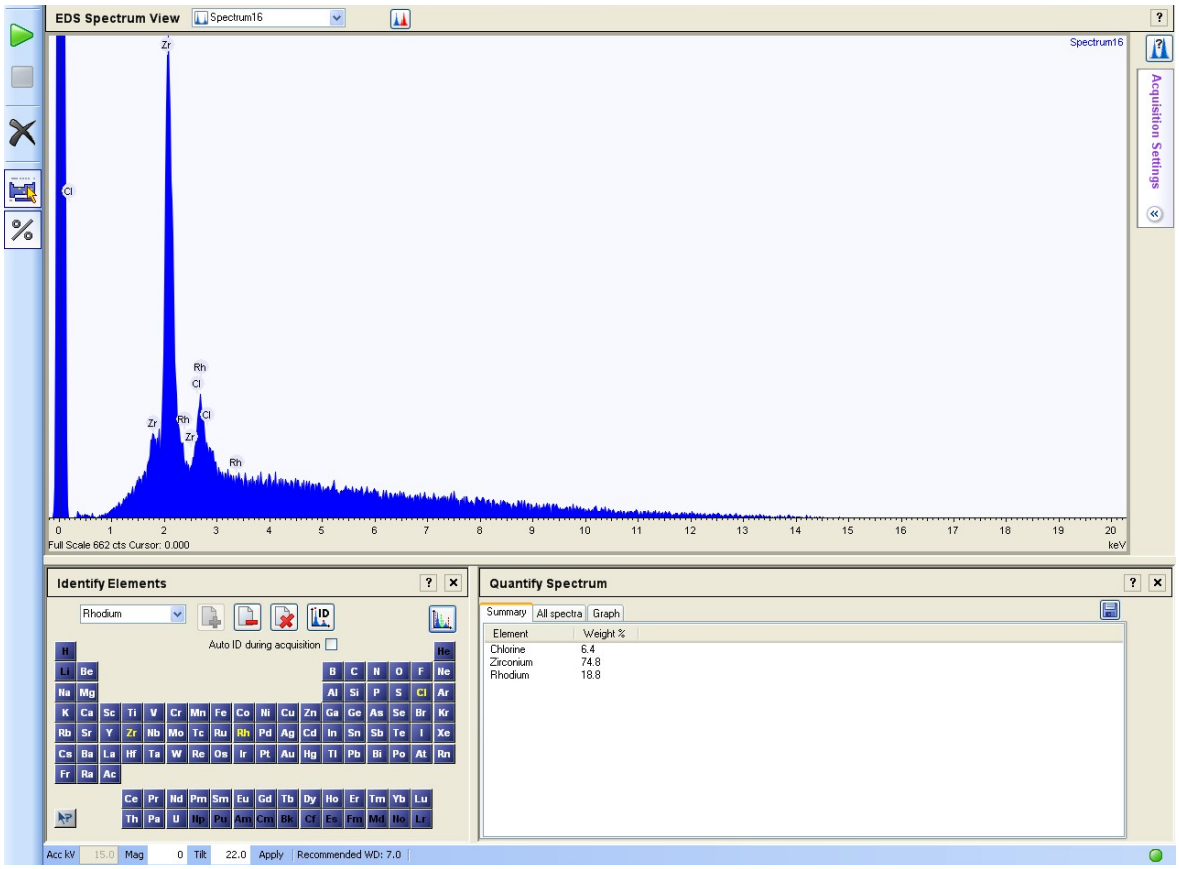

Figure S2. Energy dispersive spectra of PCN-224(Rh).

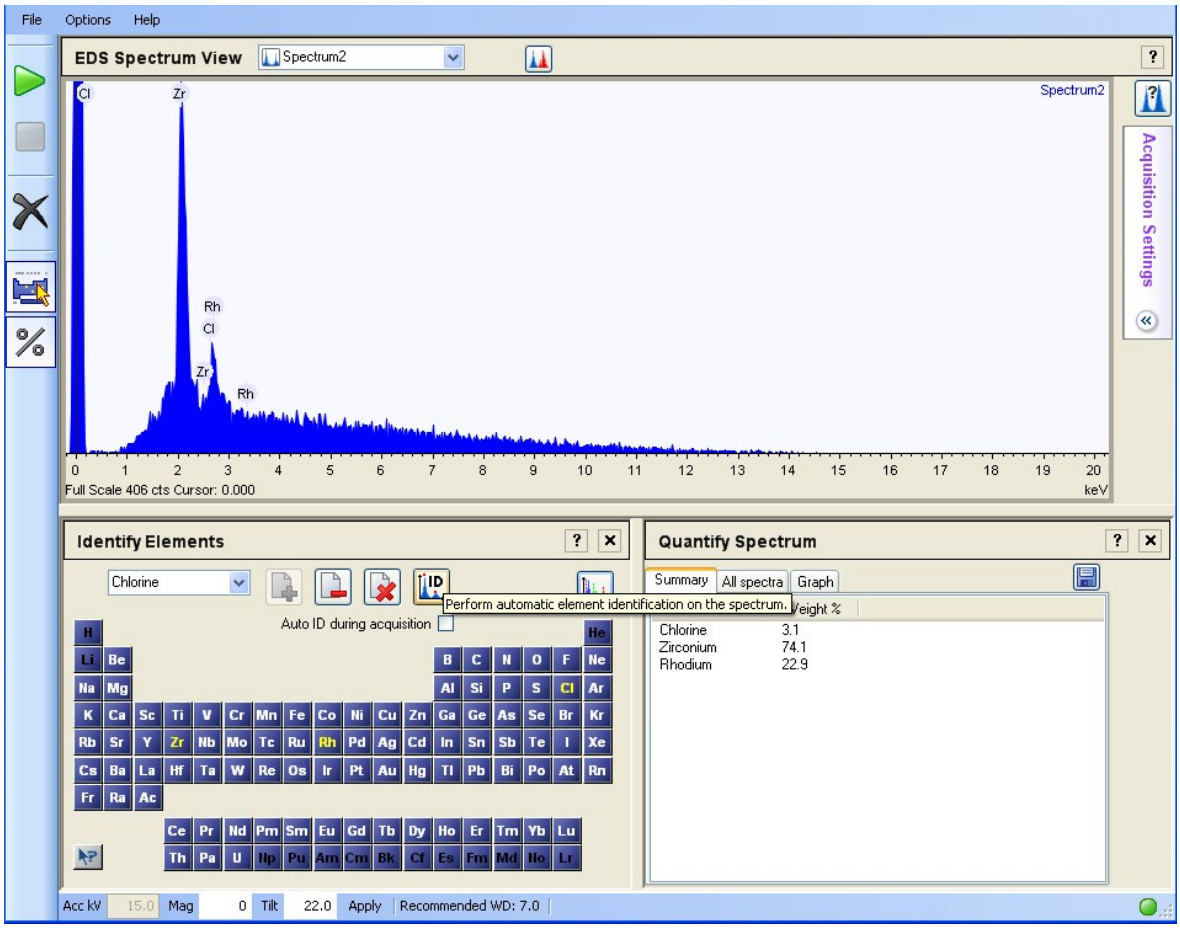

Figure S3. Energy dispersive spectra of PCN-222(Rh).

Table S1. Experimental Zr:Rh ratios in PCN-224/222(Rh).

MOF	Zr:Rh (calc.)	Zr:Rh (found)
PCN-224(Rh)	78:22	75:19
PCN-222(Rh)	73:27	74:23

3. Powder X-Ray Diffraction (PXRD)

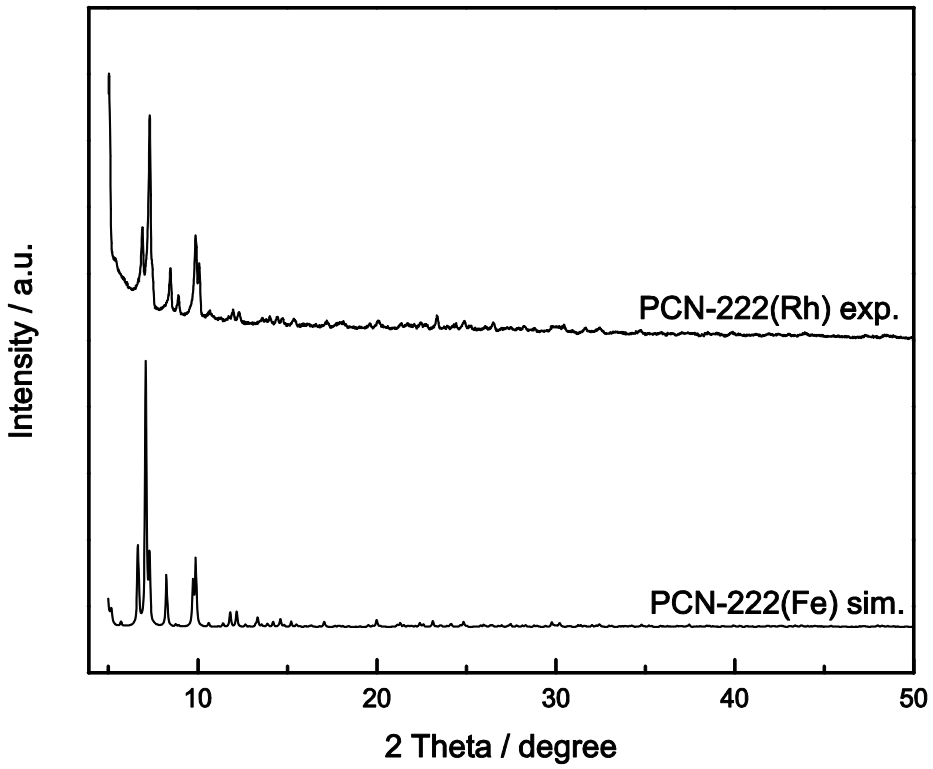

Figure S4. Experimental PXRD pattern of PCN-222(Rh) in comparison to the simulated pattern of PCN-222(Fe).

4. Pore size comparison

Table S2. Comparison of BET surface areas, pore size distributions and pore volumes of the investigated Rh-metalated MOFs with their non-metalated analogs.

MOF	BET SA (m^2/g)	PSD (nm)	Pore Volume (cm^3/g)
PCN-224(Ni)[1]	2600	1.9	1.59
PCN-224	2147	1.1, 2.1	1.10
PCN-224(Rh)	1400	1.0, 1.9	0.68
PCN-222[2]	2223	1.3, 3.2	1.31
PCN-222	2204	1.2, 3.0	1.26
PCN-222(Rh)	1912	1.2, 2.9	1.14

[1] Calculated total pore volume of PCN-224 taken from reference Feng et al., *J. Am. Chem. Soc.* **2013**, 135, 17105−17110.

[2] Experimental total pore volume of PCN-222 taken from reference Feng et al., *Angew. Chem. Int. Ed.* **2012**, 51, 10307 –10310.

5. Pore size distribution (PSD)

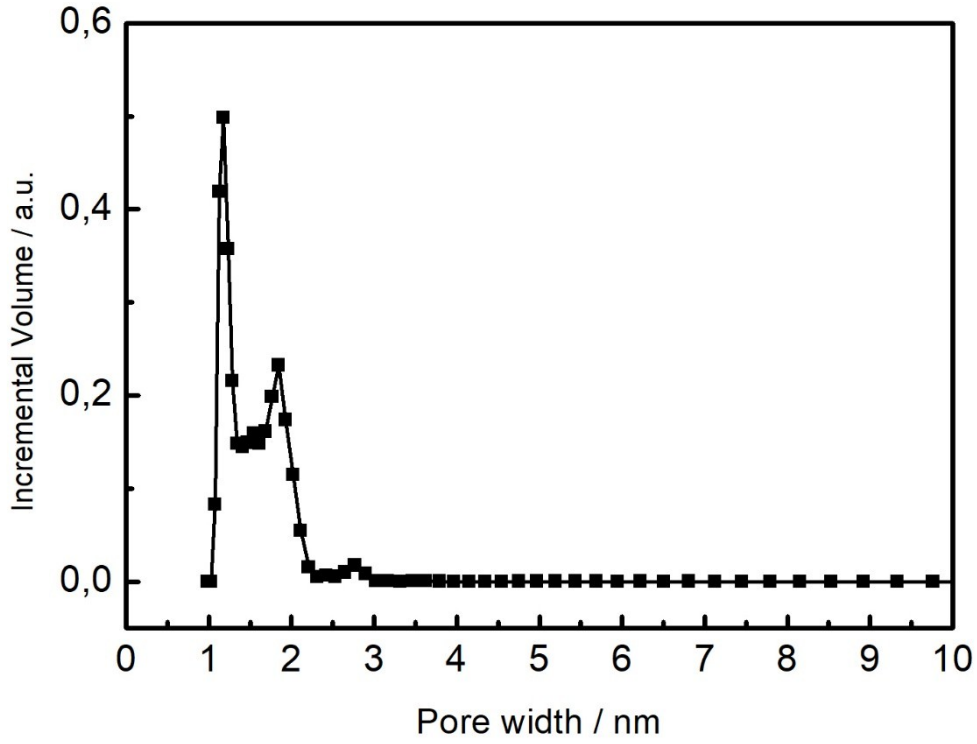

Figure S6. Pore size distribution of PCN-224(Rh).

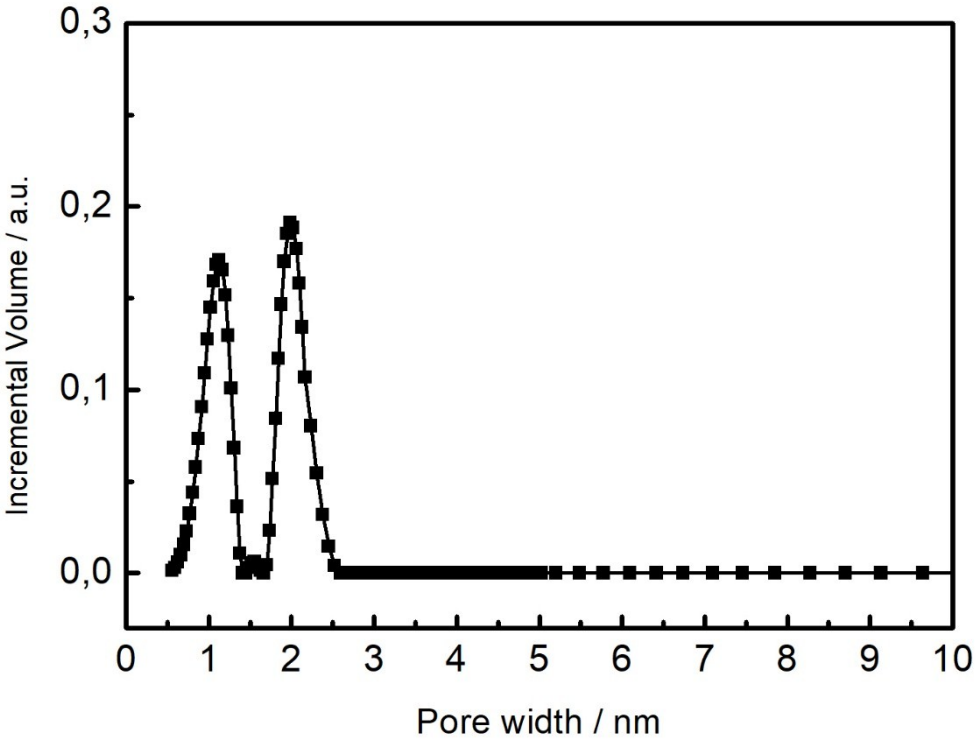

Figure S7. Pore size distribution of PCN-224.

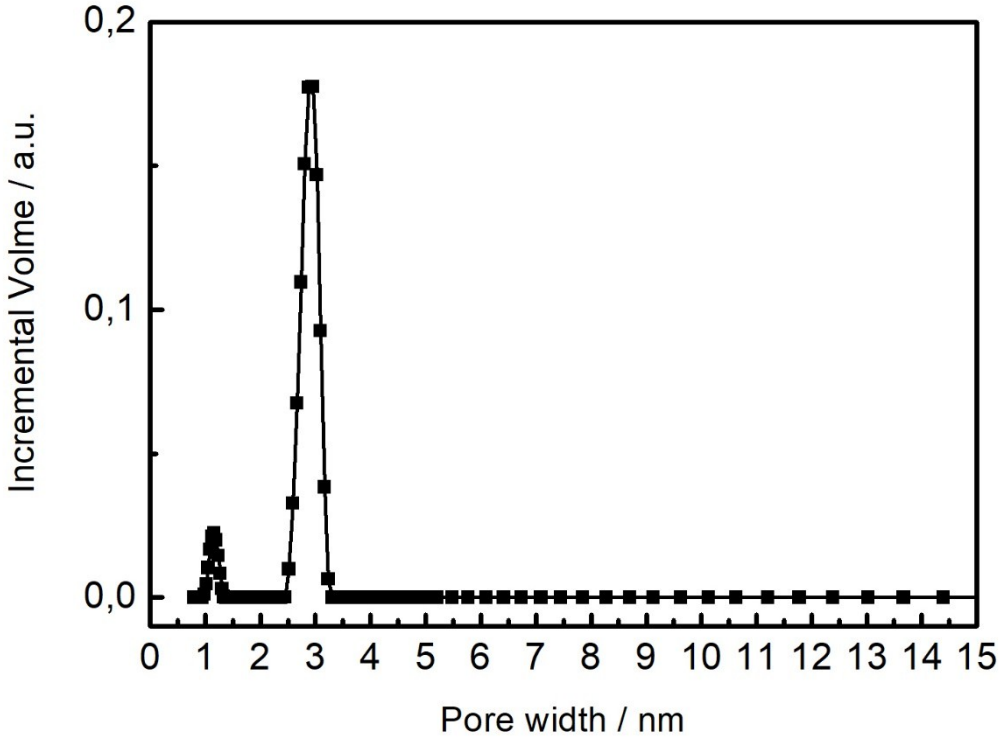

Figure S8. Pore size distribution of PCN-222(Rh).

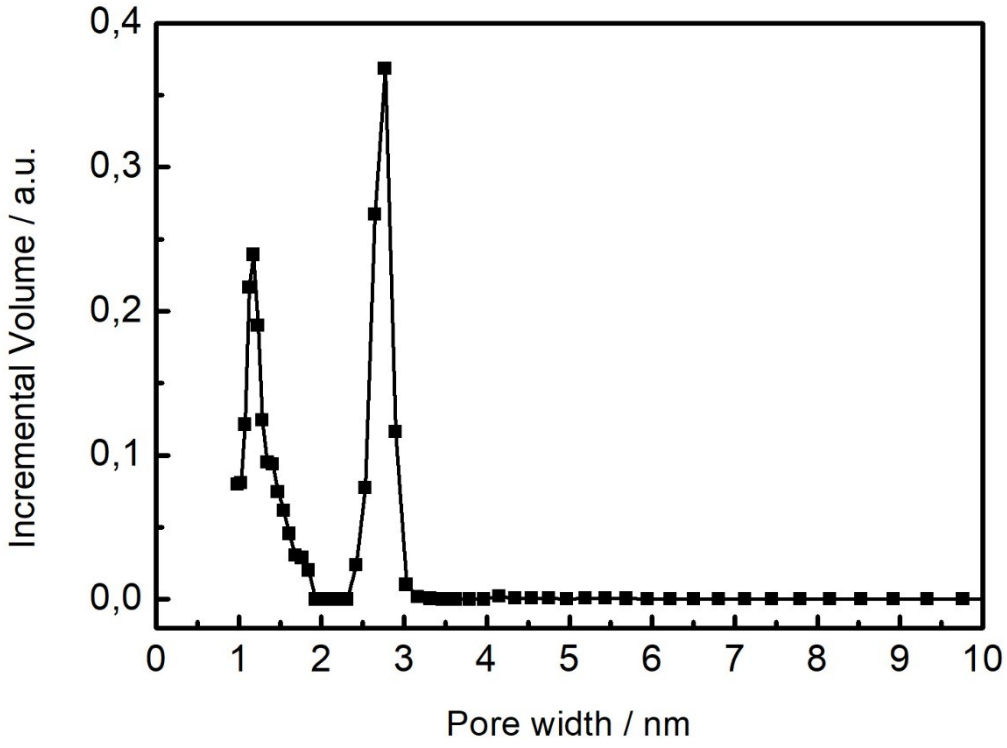

Figure S9. Pore size distribution of PCN-222.

6. Nuclear magnetic resonance (NMR)

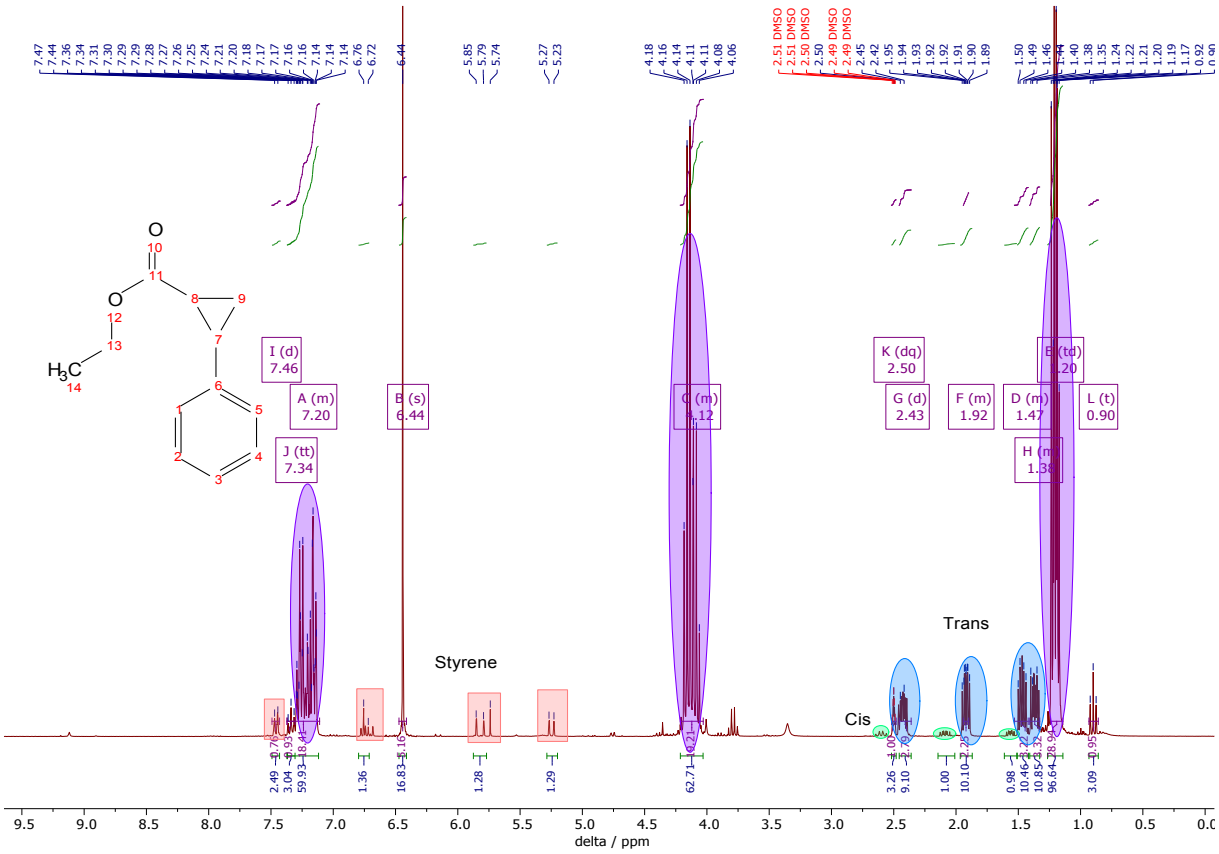

Figure S10. ^{1}H NMR spectra in DMSO-d_6 after CP reaction of styrene and ethyl diazoacetate. The chemical shifts of the *cis* and *trans* cyclopropanation products are marked in green and blue, respectively. Chemical shift coming from both products are highlighted in violet. Red marked areas indicate residual styrene.

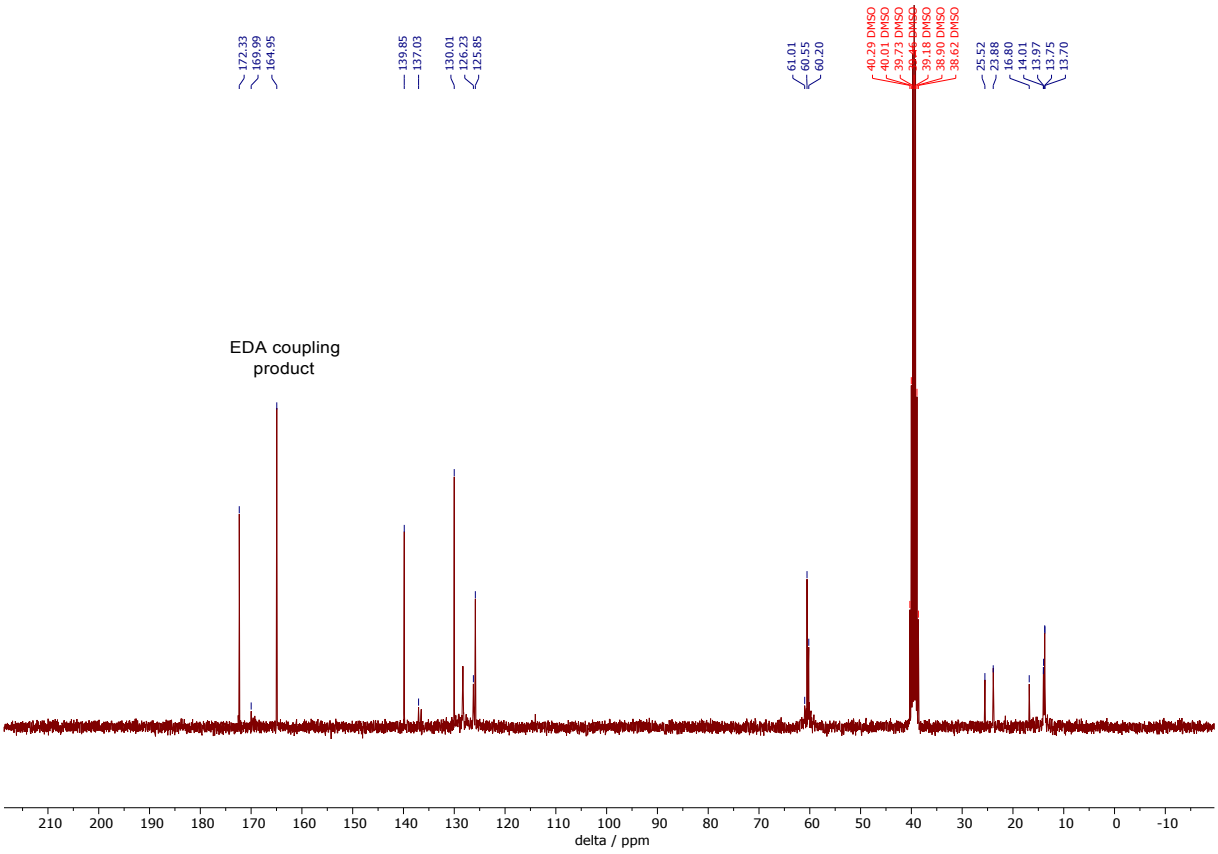

Figure S11. ^{13}C NMR spectra in DMSO-d_6 after CP reaction of styrene and ethyl diazoacetate showing *cis* and *trans* cyclopropanation products, whereby the cis cyclopropanation product is almost not visible due to the low content in the reaction mixture.

7. Graphical Illustration of the Transition States: *syn*- vs. *anti*-Product

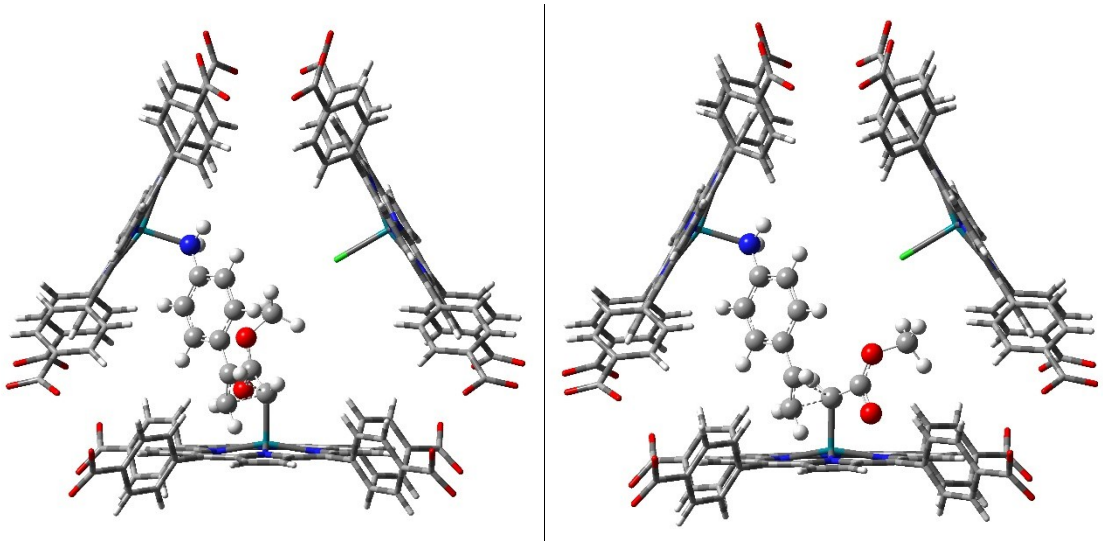

Figure S12. Graphical illustration of both transition states[a)] for the cyclopropanation of 4-aminostyrene (PCN-222(Rh)) yielding either the *syn*- (left) or the *anti*-product (right). Aminostyrene and the simplified carbene moiety (methyldiazo ester) are tentatively oriented in order to demonstrate the steric hindrance of the TS yielding the *syn*-product. [a)]The PCN-222(Rh) structure is derived from the crystallographic data whereat the Zr-oxo clusters are omitted for clarity. The organic compounds are optimized by DFT (B97D3/def2SVP, ECPstutt for Rh). Visualized by GaussView 6.0.

All calculations have been performed with Gaussian-16.B.01[1] using the B97 functional[2] with the Grimme's D3BJ dispersion[3] and the split valence basis set def2-SVP.[4] Rh atoms have been treated with the Stuttgart/Dresden 1997 relativistic effective core potential (ECP). Optimizations were obtained without using constraint coordinates.

[S1] M. J. Frisch, G. W. Trucks, H. B. Schlegel, G. E. Scuseria, M. A. Robb, J. R. Cheeseman, G. Scalmani, V. Barone, G. A. Petersson, H. Nakatsuji, X. Li, M. Caricato, A. V. Marenich, J. Bloino, B. G. Janesko, R. Gomperts, B. Mennucci, H. P. Hratchian, J. V. Ortiz, A. F. Izmaylov, J. L. Sonnenberg, Williams, F. Ding, F. Lipparini, F. Egidi, J. Goings, B. Peng, A. Petrone, T. Henderson, D. Ranasinghe, V. G. Zakrzewski, J. Gao, N. Rega, G. Zheng, W. Liang, M. Hada, M. Ehara, K. Toyota, R. Fukuda, J. Hasegawa, M. Ishida, T. Nakajima, Y. Honda, O. Kitao, H. Nakai, T. Vreven, K. Throssell, J. A. Montgomery Jr., J. E. Peralta, F. Ogliaro, M. J. Bearpark, J. J. Heyd, E. N. Brothers, K. N. Kudin, V. N. Staroverov, T. A. Keith, R. Kobayashi, J. Normand, K. Raghavachari, A. P. Rendell, J. C. Burant, S. S. Iyengar, J. Tomasi, M. Cossi, J. M. Millam, M. Klene, C. Adamo, R. Cammi, J. W. Ochterski, R. L. Martin, K. Morokuma, O. Farkas, J. B. Foresman, D. J. Fox, Wallingford, CT, **2016**.

[S2] S. Grimme, *J. Comput. Chem.* **2006**, *27*, 1787-1799.

[S3] S. Grimme, S. Ehrlich, L. Goerigk, *J. Comput. Chem.* **2011**, *32*, 1456-1465.

[S4] F. Weigend, R. Ahlrichs, *PCCP* **2005**, *7*, 3297-3305.

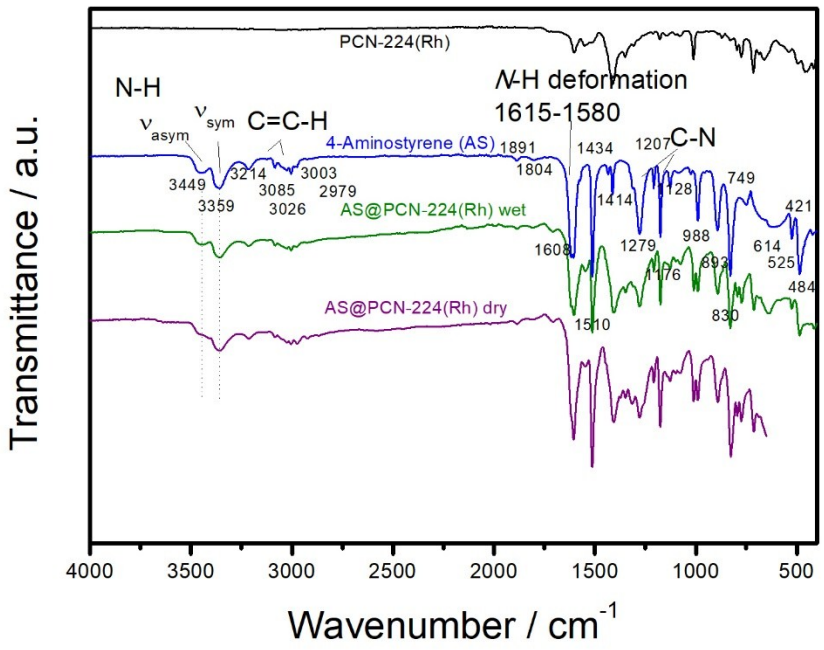

8. Infrared spectroscopy

Figure S13. Infrared spectroscopy of PCN-224(Rh) (black), 4-aminostyrene (AS, blue), AS@PCN-224(Rh) wet (high concentration of AS) and AS@PCN-224(Rh) dry (low concentration of AS).

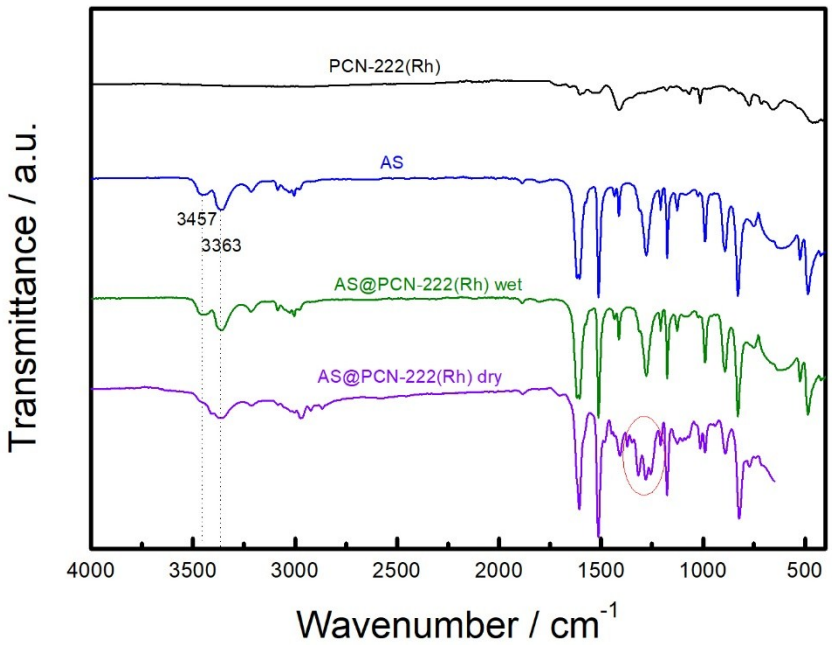

Figure S14. Infrared spectroscopy of PCN-222(Rh) (black), 4-aminostyrene (AS, blue), AS@PCN-222(Rh) wet (high concentration of AS) and AS@PCN-222(Rh) dry (low concentration of AS).